SqueezeNeRF: Further factorized FastNeRF for memory-efficient inference

Krishna Wadhwani
Sony Group Corporation
krishna.a.wadhwani@sony.com

Tamaki Kojima
Sony Group Corporation
tamaki.kojima@sony.com

Abstract

Neural Radiance Fields (NeRF) has emerged as the state-of-the-art method for novel view generation of complex scenes, but is very slow during inference. Recently, there have been multiple works on speeding up NeRF inference, but the state of the art methods for real-time NeRF inference rely on caching the neural network output, which occupies several giga-bytes of disk space that limits their real-world applicability. As caching the neural network of original NeRF network is not feasible, Garbin et.al. proposed "FastNeRF" which factorizes the problem into 2 subnetworks - one which depends only on the 3D coordinate of a sample point and one which depends only on the 2D camera viewing direction. Although this factorization enables them to reduce the cache size and perform inference at over 200 frames per second, the memory overhead is still substantial. In this work, we propose SqueezeNeRF, which is more than 60 times memory-efficient than the sparse cache of FastNeRF and is still able to render at more than 190 frames per second on a high spec GPU during inference.

1. Introduction

Image-based rendering and novel view synthesis are fundamental problems in computer vision, and there is a rich and long history of research works in these directions [2–4]. This field of novel view synthesis, using a set of observed images of a scene to recover 3D representation of the scene that allows rendering from unobserved viewpoints, has seen an unprecedented rise in popularity with the proposal of Neural Radiance Fields (NeRF) [12]. Given a limited amount of images of a scene, NeRF learns an implicit volumetric representation of the scene that allows photo-realistic rendering of novel views of the scene that is able to capture fine level details and view-dependent effects. Essentially, it is a multi-layer perceptron (MLP) based model to learn a mapping of 5D input-3D coordinates plus 2D viewing directions to density and color values. The model is optimized on a set of training views of a scene with known camera poses. The learnt model can then be used to render novel
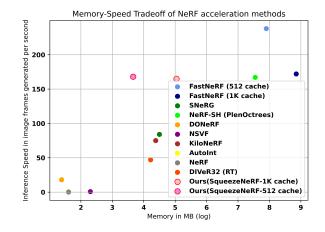

Figure 1. Memory requirement vs inference speed (to generate 800x800 image) for faster inference based NeRF models on the synthetic 360° dataset [12]. Note: Reported numbers in this figure may have different GPU settings. FastNeRF result uses Nvidia RTX-3090 while PlenOctrees and SqueezeNeRF have been tested on Nvidia V100.

views by volume rendering.

However, despite impressive view generation results, NeRF has several limitations. Some of them are: (i) it cannot handle dynamic objects and scene appearance(s), (ii) it cannot handle unbounded scenes, (iii) a network trained on one scene cannot generalize across another scene, (iv) it requires relatively large number of views to learn an accurate representation, and (v) slow inference speed. These several limitations of NeRF have inspired several follow-up works such as [1, 5, 19, 20].

In this work, we focus on the slow rendering issue of NeRF. The reason why NeRF is slow during inference is also, its greatest strength - an MLP-based volumetric representation. How NeRF works is that for a given camera pose, a ray is projected that passes through each pixel in the image into the 3D scene. We then sample points on each ray, predict the color and density value at each point and then, do volumetric integration along each ray to compute the final color at the pixel location. While the simplicity of NeRF's representation of a 3D scene via a MLP is elegant

and results in high-quality novel view synthesis of a scene, it also means that during inference, we need to query the neural network to get the color and density values for millions of points. For example, in order to render a 800x800 image by sampling 192 points along each ray, we will need to query the neural network for 122.88 million 3D points. This means that it takes a several seconds to render an image via NeRF on a high-end GPU.

There have been multiple works that have attempted to speed-up NeRF inference [6–10, 14, 17, 18]. While all of them are considerably faster than the original NeRF model during inference, they either still do not achieve real time rendering [8–10] or achieve real-time rendering at the cost of significant memory overhead [6, 7, 17, 18].

The state-of-the-art approaches in speeding up NeRF inference rely on caching the mapping learnt by MLP. Now it must be stated that caching the original NeRF model is not practically possible. This is because NeRF maps a 5-dimensional input (3D coordinate p + 2D viewing direction d) to a 4-dimensional output (RGB color c and scalar density σ). So caching this function in the input space would mean that the cache-size would scale with n^5 (where n is the number of bins or sampled values per input dimension). For $n = 512$ bins per input dimension, the cache size would be approximately 176 terabytes and infeasible to store. In order to solve this issue, FastNeRF [6] proposed a novel architecture that factorizes the problem into 2 independent networks - their first MLP takes the 3D coordinate p as input and the second MLP takes the 2D viewing direction d as input. The outputs of these two networks are combined via their inner product to produce the RGB color values. Now considering n_p number of bins for each position dimension and n_d number of bins for each viewing direction component, the FastNeRF cache size would have a complexity of $\mathcal{O}(D_p n_p^3 + D_d n_d^2) \sim \mathcal{O}(n^3)$ where D_p and D_d represent the dimensionality of the position dependent MLP output and viewing direction dependent MLP output respectively. For standard FastNeRF configuration of $D_p = 25, D_d = 8$ and $n_p = 512, n_d = 256$, the cache size is approximately 6.7 GB, if all the values are stored as half-precision floating point numbers. The FastNeRF authors further leveraged the scene sparsity to store a sparse cache instead of a dense one in order to reduce the cache size to around 3GB. Similarly, NeRF-SH [18] and SNeRG [7] also use an architecture based on similar factorization but rely on different architecture and cache-storage strategy.

While FastNeRF and NeRF-SH (PlenOctrees based inference) can render over 150 frames per second (FPS) on a high-end GPU, their cache takes up several gigabytes (GBs) of memory, which make them prohibitive for any embedded system application and can lead to memory fragmentation issues during inference. Moreover, as a NeRF requires a different MLP to be trained for each scene, storing several GBs of cache for every scene makes this memory overhead issue even worse.

To address this issue, we propose SqueezeNeRF, a further factorized version of FastNeRF which is able to render over 150 FPS with affordable cache-size. This makes the model convenient for deploying on embedded systems. SqueezeNeRF factorizes the position dependent MLP of FastNeRF into 3 separate MLPs - which take $(x, y), (y, z)$ and (z, x) as input. This factorization enables SqueezeNeRF to have a cache-size complexity of $\mathcal{O}((D_{p_{xy}} + D_{p_{yz}} + D_{p_{zx}})n_p^2 + D_d n_d^2) \sim \mathcal{O}(n^2)$, where $D_{p_{xy}}, D_{p_{yz}}, D_{p_{zx}}$ represent the dimensionality of the 3 position dependent networks. For a standard SqueezeNeRF configuration of $D_{p_{yz}} = D_{p_{yz}} = D_{p_{yz}} = 25, D_d = 8$ and $n_p = 512, n_d = 64$, the cache-size is approximately 40 MB, which is more than 160 times memory efficient than the dense FastNeRF cache, more than 65 times memory efficient that sparse FastNeRF cache. We further compare our approach with the fast inference based NeRF approaches in terms of performance, speed and memory requirements and show that our relatively straightforward approach is competitive with the state-of-the-art approaches in terms of speed while being more memory-efficient, although is slightly inferior in terms of image generation performance.

The contributions of our work can be summarized as:

- We propose SqueezeNeRF, which is the first approach that allows NeRF rendering at over 150 frames per second with cache-size less than 200 megabytes. The approach is based on a novel NeRF architecture, that is based on further factorization of FastNeRF.

- We present a comprehensive evaluation of NeRF follow-up works for faster inference and compare their speed, performance and memory requirements.

2. Related Work

Neural Radiance Fields [12] has shown impressive results in the task of novel view generation of a static scene but is limited by its slow inference speed. A number of recent works [6–10, 14, 16, 18] have tried to address this particular limitation of NeRF. Our proposed model, SqueezeNeRF also belongs to these family of methods aimed to improve the inference speed of NeRF.

AutoInt [9] proposed a neural network to learn integrals along each ray with reduces number of point samples on each ray. Neural Sparse Voxel Fields [10] learns a sparse voxel grid that allows to skip over empty region during inference. While considerably faster than NeRF, [9,10] do not render at interactive frame rates.

KiloNeRF [14] splits one network into multiple tiny networks and parallelizes the multiple network evaluations. DIVeR [17] combines implicit representation learning with

voxel based representation and uses deterministic integration instead of the sampling scheme done in NeRF. DON-eRF [13] predicts depth distribution along each ray for using reduced number of samples in volumetric rendering. NeX [16] models the scene as a multi-plane image (MPI) rather than a continuous volumetric representation. While NeX shows impressive results, it cannot model scenes where the viewpoint span is high. State-of-the-art methods [6,7,18] in fast inference of NeRF rely on caching the neural network output. Caching NeRF MLP is not feasible due to extremely high memory complexity. So all these work modify the NeRF architecture in order to make this caching possible. All [6,7,18] factorize the structure of the implicit model, by using two separate neural networks for 3D position and camera view direction. While this factorization allows their network cache to be 1000 times smaller than NeRF and perform inference at interactive rate, their cache-size is still in the order of few giga-bytes. Although memory requirement in [7, 13, 14, 17] is smaller due to not relying on cache [13, 14] or efficient compression scheme [7], their rendering speed is less than those in FastNeRF [6] and NeRF-SH [18]. In this work, we further factorize the position dependent network in FastNeRF which allows us to reduce the FastNeRF cache-size by more than 60 times as compared to FastNeRF or NeRF-SH, while still maintaining similar rendering speed.

A concurrent work [8] also proposed to combine implicit representation based learning neural networks with a split MLP architecture, which is similar in spirit to the idea of factorization used by FastNeRF or us. They use a separate MLP for each dimension of the input but they do not employ caching for faster inference and their speed-up for inference is significantly less than our approach.

3. Method

In this section, we describe SqueezeNeRF. FastNeRF splits NeRF into 2 neural networks - a position (x, y, z) dependent network and viewing direction dependent network. The key idea in this work is to further split the position dependent network into 3 networks, which are dependent on (x, y), (y, z) and (z, x) respectively. We briefly recap NeRF and FastNeRF in the following subsection before describing the details of our model.

3.1. Background

Neural Radiance Fields (NeRF): Given multi-view images of a scene with known camera poses and parameters, NeRF [12] learns to recover the 3D volumetric representation of a scene in the form of (i) opacity field or volume density σ that captures a soft or an approximate geometry of the scene and (ii) a radiance field or RGB color c that captures the view dependent surface texture. This representation is captured in the form of a mapping from 3D co-

ordinate position $p = (x, y, z)$ and 2D viewing direction $d = (\theta, \phi)$. A MLP F_{NeRF} is used to learn this mapping $F_{NeRF} : (p, d) \rightarrow (\sigma, c)$. The density σ is modelled as a function of p. On the other hand, the color c is modelled as a function of both p and d.

How this process works is that for a given viewing angle, in order to render a single pixel at pixel location P, a ray is projected from the camera center that passes through that pixel and into the 3D scene. This ray direction is denoted as d. N number of 3D points are sampled along this ray $(p_1, p_2 \ldots p_N)$ between the near and far plane of the camera. Each point sample is fed as input to the neural network which then predicts the color c_i and density σ_i at each point p_i. The color and density value at each point is then used to compute the final pixel color $\hat{c}$ using volumetric integration as:

$$\hat{c}(P) = \sum_{i=1}^{N} T_i(1 - \exp(-\sigma_i \delta_i) c_i), \quad (1)$$

where $T_i = \exp(-\sum_{j=1}^{i-1} \sigma_j \delta_j)$ is the transmittance and $\delta_i = (p_{i+1} - p_i)$ is the distance between adjacent samples.

Given a set of training images with known camera poses, NeRF optimizes the MLP by minimizing the squared error between input pixel color and the pixel color value predicted using Eq. (1). So, the network weights are trained to optimize:

$L_p = \sum_P ||c(P) - \hat{c}(P)||_2^2$,

where $c(P)$ is the ground truth color at P. Hence, by replacing an explicit volumetric representation with an MLP, NeRF requires orders of magnitude less space than a dense voxel grid, but rendering an image requires querying the neural network at millions of 3D points, which makes the rendering process slow and computationally expensive.

FastNeRF: As mentioned earlier, FastNeRF [6] splits NeRF's neural network F_{NeRF} into two networks, (i) position dependent network $F_{pos} : p \rightarrow \{\sigma, (u, v, w)\}$ and (ii) ray direction dependent network $F_{dir} : d \rightarrow \beta$ where u, v, w are D-dimensional vectors that form a radiance map describing the view dependent radiance at position p, and β is a D−dimensional vector for the D components of the deep radiance map. Note that D is a hyperparameter here and is set as 8 for most of the scenes in FastNeRF and this work as well. The color at a given 3D position is then computed by taking the inner product of the weights and deep radiance map:

$$c = (r, g, b) = \sum_{i=1}^{D} \beta_i(u_i, v_i, w_i) = \beta^T \cdot (u, v, w). \quad (2)$$

After computing the color c at a given 3D position, the final pixel color can be computed in a similar manner as NeRF by using Eq. (1).
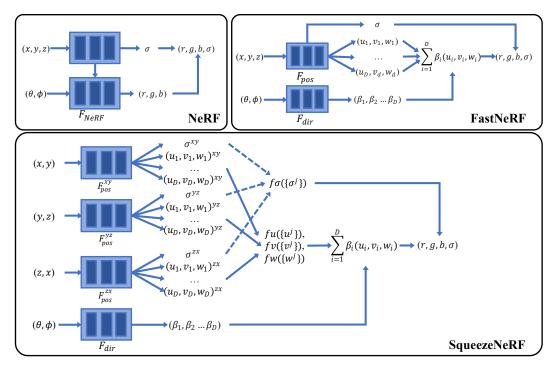
Figure 2. **Neural network architecture comparison.** Top left: NeRF architecture. Cache-size of the original NeRF network is of the order $\mathcal{O}(n^5)$, where n is the number of bins per input dimension. Top right: FastNeRF [6] architecture based on factorization into position dependent network F_{pos} and F_{dir}. Cache-size of FastNeRF network is of the order $\mathcal{O}(n^3)$. Bottom: Proposed SqueezeNeRF architecture that further factorizes the position dependent network in FastNeRF into 3 networks: F_{pos}^{xy}, F_{pos}^{yz} and F_{pos}^{zx}. Cache-size of SqueezeNeRF network is of the order $\mathcal{O}(n^2)$. In the above diagram, (x, y, z) denotes 3D position of input sample, (θ, ϕ) denotes camera ray direction and (r, g, b, σ) are the color and density/opacity values.

3.2. SqueezeNeRF

Default architecture: In our proposed SqueezeNeRF, we further split F_{pos} into three networks as:

$F_{\text{pos}}^j : j \rightarrow \{(\sigma_0^j, W_\sigma^j), (\boldsymbol{w}_{\boldsymbol{u}}^j, \boldsymbol{u}_0^j, \boldsymbol{w}_{\boldsymbol{v}}^j, \boldsymbol{v}_0^j, \boldsymbol{w}_{\boldsymbol{w}}^j, \boldsymbol{w}_0^j)\}$, for $\forall\ j \in \{(x, y), (y, z), (z, x)\}$.

We then compute $\sigma^j, \boldsymbol{u}^j, \boldsymbol{v}^j$ and $\boldsymbol{w}^j$ ($*$ denotes pointwise multiplication) as:

$$\sigma^j = \sigma_0^j * w_\sigma^j, \boldsymbol{k}^j = \boldsymbol{w}_{\boldsymbol{k}}^j * \boldsymbol{k}_0^j\ \forall\ \boldsymbol{k} \in \{\boldsymbol{u}, \boldsymbol{v}, \boldsymbol{w}\}. \quad (3)$$

Essentially for each σ^j and $\boldsymbol{k}^j$, we also compute its corresponding weight. In our experiments, we found that explicitly predicting the weight of the quantities and then, using them for subsequent computation Eq. (4) led to better results. We also present the non-weighted network performance as an ablation study in Tab. 5.

We then combine the output of the three networks:

$$\sigma = f_\sigma(\{\sigma^j\}), \boldsymbol{k} = f_{\boldsymbol{k}}(\{\boldsymbol{k}^j\})\ \forall\ \boldsymbol{k} \in \{\boldsymbol{u}, \boldsymbol{v}, \boldsymbol{w}\}, \\ \forall\ j \in \{(x, y), (y, z), (z, x)\}. \quad (4)$$

There can be multiple ways in which we represent the network outputs. In the default SqueezeNeRF configuration, for simplicity, we model each σ^j as a scalar value and

each $\boldsymbol{k}$ as a D dimensional vector ($w_\sigma^j \in \mathcal{R}, \boldsymbol{w}_{\boldsymbol{k}}^j \in \mathcal{R}^D$). We use a straightforward combination scheme to model $f_\sigma, f_{\boldsymbol{k}}$ as represented in Fig. 2. We simply multiply all σ^j to get our final σ value. We add each $\boldsymbol{k}^j$ to get $\boldsymbol{k}$.

Alternate architecture: We also evaluate our factorization scheme with another type of architecture. Referred to as "SqueezeNeRF (alt)" in our results, F_{pos} is split as

$F_{\text{pos}^j} : j \rightarrow \{\boldsymbol{\sigma}^j, \boldsymbol{u}^j, \boldsymbol{v}^j, \boldsymbol{w}^j\}$.

Here each $\boldsymbol{\sigma}^j \in \mathcal{R}^{D_\sigma}$ and $\boldsymbol{k} \in \mathcal{R}^{D_{\boldsymbol{k}}}$. In our experiments, D_σ is set as 12 and $D_{\boldsymbol{k}}$ is set as 8. Finally σ and $(\boldsymbol{u}, \boldsymbol{v}, \boldsymbol{w})$ is computed as:

$$\sigma = W_\sigma[\text{concat}(\{\boldsymbol{\sigma}^j\})] + b_\sigma, \\ \boldsymbol{k} = W_{\boldsymbol{k}}[\text{concat}(\{\boldsymbol{k}^j\})] + b_{\boldsymbol{k}}, \quad (5)$$

where $W_\sigma \in \mathcal{R}^{1 \times 3D_\sigma}, b_\sigma \in \mathcal{R}, W_{\boldsymbol{k}} \in \mathcal{R}^{D \times 3D_{\boldsymbol{k}}}, b_{\boldsymbol{k}} \in \mathcal{R}^D$ are learnable parameters, that are also saved when the neural network is cached and concat refers to concatenation operation.

Please note that while other factorization schemes such as splitting (x, y, z) into x, y, z instead of $(x, y), (y, z)$ and (z, x) is also possible but, we found that the former factorization scheme lead to considerably inferior results. Experimentation with more sophisticated combination functions

in Eq. (4) is left as part of future work.

F_{dir} remains same as that in FastNeRF. After computing $\sigma, (\boldsymbol{u}, \boldsymbol{v}, \boldsymbol{w})$, we follow Eq. (2) to compute the color at a 3D point sample and then use Eq. (1) to compute the final pixel color. After computing the final pixel color, SqueezeNeRF is trained in a similar manner as NeRF.

3.3. Caching

The motivation of our proposed architecture is that the cache-size of the mapping learnt by all the F_{pos}^j and F_{dir} is considerably small. Following similar caching strategy as described in FastNeRF, we define a bounding box that covers the entire scene captured by the NeRF. We sample n_p values along each 3D dimension and n_d number of points for each of the ray direction coordinate θ and ϕ. Hence for each F_{pos}^j, we store the output of n_p^2 values, that is, we store $\{\,\sigma^j,\,(\boldsymbol{u}^j,\,\boldsymbol{v}^j,\,\boldsymbol{w}^j)\,\}$ for every ordered pair of j. For default architecture, σ^j is a scalar value and $(\boldsymbol{u}^j,\,\boldsymbol{v}^j,\,\boldsymbol{w}^j)$ are D dimensional vectors, we store $3n_p^2(3D+1)$ values for n_p^3 combination of (x, y, z). Similarly for SqueezeNeRF (alt), we store $3n_p^2(3D + D_\sigma)$ values for n_p^3 combination of (x, y, z). For F_{dir}, we store the output for D dimensional vector for the n_d^2 combination of (θ, ϕ). So, we store $n_d^2(D)$ output values of F_{dir}.

In our experiments, we observe that $n_d = 64$ for synthetic 360° [12] and $n_d = 32$ for LLFF dataset [11] is sufficient for good results. We further test the cache based inference model for $n_p = 512$ (referred to as 512 cache) and $n_p = 1024$ (referred to as 1K cache). Based on our experimental observations, we store each σ^j using 32 bit floating point precision whereas each of $\boldsymbol{u}^j, \boldsymbol{v}^j, \boldsymbol{w}^j$ and $\boldsymbol{\beta}$ are stored using 16 bit floating point precision. In total, our 1K cache takes up 155MB of memory whereas our 512 cache occupies 39MB. A similarly dense 1K cache for FastNeRF would take approximately 54GB, and the corresponding 512 cache would occupy approximately 6.7GB. Also, the corresponding 1K cache and 512 cache size for NeRF would be approximately 35TB and 4.4TB respectively. Alternatively, SqueezeNeRF (alt) is evaluated with $n_p = 512, n_d = 256$ and all the values are stored using 16 bit floating point precision. So, the 512 cache for SqueezeNeRF (alt) occupies 58MB. Readers are referred to the Supplementary of [6] for the formulas used to calculate cache sizes for FastNeRF and NeRF. The formula was similarly adapted for cache-size calculation of SqueezeNeRF.

Also note that as the dense cache corresponding to Fast-NeRF, NeRF-SH [18] and SNeRG [7] are quite huge, they save a sparse cache of the neural network mapping based on the scene geometry. While this works fine in case of the scenes used for comparison in this and their work, we believe that this will be less effective for highly dense and feature-rich scenes. On the other hand, SqueezeNeRF enables storage of affordable dense cache.

3.4. Implementation

The SqueezeNeRF training script is based on that of NeRF [12]. Apart from the different architecture, the training process is identical to NeRF.

The position dependent MLPs are modelled using 6 layers with 256 hidden units each whereas the view dependent MLP is modelled with 4 layers and 128 hidden units. As our network has more number of parameters than NeRF, it's training and inference without caching the trained network is slower than that of NeRF. Other training features such as hierarchical sampling and positional encoding and training and testing hyper-parameters are same as that in NeRF.

At inference, similar to NeRF, our method takes a test view as input and predicts the color at each pixel location as described in Sec. 3.2. We sample 256 points along each projected ray. The 3D location and viewing direction of each point is then used to fetch $\sigma^j, \boldsymbol{u}^j, \boldsymbol{v}^j, \boldsymbol{w}^j, \boldsymbol{\beta}$ from the respective cache files, which are then used to compute the color and density using Eq. (4) and Eq. (2). Finally, the final pixel color is computed using Eq. (1).

While we use custom CUDA kernels for speeding up inference, our implementation relies on simply querying our dense cache and computing the pixel color via ray marching. We use nearest neighbour interpolation for cache lookup of the outputs of F_{pos}^j and bilinear interpolation for sampling from the cache of F_{dir}

Unlike FastNeRF, we did not use bounded volume hierarchy based ray tracing or other performance enhancements. Therefore, the performance of our approach can be further improved with similar techniques.

4. Experiments, Result and Discussion

We evaluate our method along with the current approaches on novel view synthesis in terms of quality of rendered images, speed at which the images are generated and memory requirement for any additional data structure such as a cache for neural network output or weights of trained neural network. We use two datasets for this task - NeRF synthetic 360° [12] and forward facing Local Light Field Fusion (LLFF) dataset [11].

Image quality: To evaluate the quality of rendered images, we quantitatively measure the performance by comparing the model output to its corresponding ground truth image in the test set using 3 metrics - Peak Signal to Noise Ratio (PSNR), Structured Similarity (SSIM) [15] and LPIPS [21]. In the top half of Tab. 1 and Tab. 2, we compare the quality of images rendered by our model (without caching) to NeRF [12], the corresponding network outputs of the different NeRF variants that also rely on caching for speeding up inference [6, 7, 18] and faster inference based NeRF models that do not rely on caching. In the bottom half, we compare the cache based inference of the different

Method	Image Generation Quality			Speed [FPS] ↑	Memory [MB] ↓
	PSNR [dB] ↑	SSIM ↑	LPIPS ↓		
NeRF [12]	30.23	0.946	0.050	0.04	**5**
FastNeRF (no-cache) [6]	29.16	0.936	0.053	0.03	28
NeRF-SH (no-cache) [18]	<u>31.57</u>	<u>0.953</u>	0.047	14	12
JAXNeRF+ Deferred [7]	30.55	0.952	0.049	0.01	18
KiloNeRF [14]	31.00	0.920	0.060	**50**	160
AutoInt (8 sections) [9]	25.55	0.911	0.170	0.6	**5**
DIVeR32 (RT) [17]	**32.12**	**0.958**	**0.033**	<u>47</u>	68
SqueezeNeRF (no-cache)	29.59	0.931	<u>0.038</u>	0.02	<u>11</u>
FastNeRF (1K Cache)	29.97	0.941	0.053	172	16200
FastNeRF (512 Cache)	N/A	N/A	N/A	**238**	2700
NeRF-SH (PlenOctree)	**31.71**	**0.958**	0.053	<u>168</u>	1900
SNeRG (PNG) [7]	<u>30.38</u>	<u>0.950</u>	<u>0.050</u>	84	<u>87</u>
SqueezeNeRF (1K Cache)	29.61	0.921	**0.046**	165	155
SqueezeNeRF (512 Cache)	28.12	0.917	0.087	<u>168</u>	**39**

Table 1. **Results: Comparison of Image Quality, inference speed and required memory for storing cache/network weights for the novel view synthesis of 800x800 image in synthetic** $360°$ **dataset.**

Method	Image Generation Quality			Speed [FPS] ↑	Memory [MB] ↓
	PSNR [dB] ↑	SSIM ↑	LPIPS ↓		
NeRF [12]	<u>26.50</u>	<u>0.855</u>	<u>0.07</u>	<u>0.06</u>	**5**
FastNeRF (no-cache) [6]	**27.96**	0.888	**0.063**	0.04	28
JAXNeRF+ Deferred [7]	24.32	0.808	0.086	0.00	18
AutoInt (8 sections) [9]	24.14	0.820	0.176	0.6	**5**
NeX [16]	27.26	**0.904**	0.178	**449**	89
SqueezeNeRF (no-cache)	24.32	0.808	0.085	0.03	<u>11</u>
SqueezeNeRF (alt, no-cache)	26.08	0.859	0.081	0.02	<u>11</u>
FastNeRF (768 Cache)	**26.04**	**0.856**	0.085	**714**	6100
SNeRG (PNG) [7]	<u>25.63</u>	<u>0.818</u>	0.183	27	373
SqueezeNeRF (1K Cache)	22.50	0.762	<u>0.122</u>	480	155
SqueezeNeRF (512 Cache)	21.62	0.729	0.189	<u>484</u>	**39**
SqueezeNeRF (alt, 512 Cache)	23.87	0.817	**0.071**	190	<u>58</u>

Table 2. **Results: Comparison of Image Quality, inference speed and required memory for storing cache/network weights for the novel view synthesis of 504x378 image in LLFF dataset.**

NeRF variants to our model's cache based inference. The reported PSNR for NeRF synthetic 360° and LLFF are averaged across all the eight types of scenes present in the two types of datasets. KiloNeRF [14], DIVeR32 [17] and NeRF-SH [18] are not designed for frontal facing and unbounded scenes so, their performance is not reported in Tab. 2. Likewise, NeX [16] is not designed for 360° scenes so its performance is not reported in Tab. 1. The reported PSNR in these tables are taken from the respective papers. From these tables, we can see that the quality of images generated by our proposed network architecture is competitive with NeRF and other models. Cache based inference does lead to a degradation in the quality of the images, but also provides significantly high rendering speed. For the NeRF synthetic 360° dataset, the drop in quality due to cache based infer- ence is still small (<7%) and the rendered images in Fig. 3 (a-b) also verify that that. For LLFF dataset, the drop in image quality is relatively higher but still, the rendered images in Fig. 3 (d-e) still look reasonable. The significant drop in the quality of images generated by SqueezeNeRF for LLFF dataset served as our motivation to propose SqueezeNeRF (alt). From the tables, we can see that the quality of images generated by SqueezeNeRF (alt) is superior to SqueezeN- eRF but the performance improvement comes at the cost of slower inference speed. With that said, with caching, we can still render at 190 FPS with SqueezeNeRF (alt).

Rendering speed comparison: We compare the infer- ence speed of our method with the baselines in terms of number of image frames generated per second. In Tab. 1 and Tab. 2, the inference speed for NeRF [12], NeRF-SH

(no-cache and plenoctree) [18], AutoInt [9] has been meaured on a single Nvidia V100 GPU. FastNeRF has been measured on Nvidia RTX 3090, while JAXNeRF+ Deferred and SNeRG have been measured on Nvidia RTX 2080 and KiloNeRF [14] and DiVeR32 [17] have been measured on Nvidia GTX 1080 Ti. For the purposes of comparison in Tab. 1, Tab. 2 and Tab. 4, we report our performance on a single Nvidia V100 GPU. We also report our inference speed on Nvidia A100 GPU in Tab. 3.

In Tab. 1 and Tab. 2, we can see that our method enables real-time inference of NeRF and is able to render at over 150 frames per second. The rendering speed of our method is competitive with the state of the art methods [6, 18], while our memory requirement is significantly less than these methods. Moreover, in Tab. 4, we also compare [6, 18] with our method in terms the time taken to generate taken to generate the cache for neural network. Our smaller cache-size allows us to generate the cache in less than 9s, in contrast to the considerably longer time required by other methods, which is another advantage of our method. So even if the inference speed of our 512 cache model is less than the corresponding FastNeRF model, it will take FastNeRF over 16 minutes to compensate for the longer cache generation time in comparison to our approach.

Memory comparison and speed-memory trade-off: In Tab. 1 and Tab. 2, we also compare the memory requirement of our method along with our baselines. For SNeRG [7], NeRF-SH (PlenOctree) [18], FastNeRF [6] cache based inference and our method, memory here refers to the network cache-size. For other methods, memory here refers to the memory occupied by the weights of the trained neural network. From the two tables, we can see that non-caching based methods have a considerably less memory overhead but have a slower inference speed compared to the caching based methods. So there is a clear trade-off between the memory efficiency of a model and it's inference speed. From Tab. 1, Tab. 2 and Fig. 1, we can see that our model can generate images at a high speed, which is competitive with caching based methods, with sufficiently low memory requirement, which is closer to the non-caching based methods.

Other experiments: In Tab. 5, we also present results of our model with different configurations. We compare the quality of image generation of our final model configuration (referred to as SqueezeNeRF (no-cache in Tab. 5) in terms of PSNR to the different configurations of hidden dimension in the MLPs of F_{pos}^{xy}, F_{pos}^{yz} and F_{pos}^{zx} and different settings of D, dimensionality of $\boldsymbol{u}, \boldsymbol{v}, \boldsymbol{w}$ and $\boldsymbol{\beta}$. In Tab. 5, we also show the effect of number of bins per dimension on the quality of images generated via cache-based inference.

Method	Cache-size [MB] ↓	Speed [FPS] ↑	
		V100	A100
SqueezeNeRF (1K cache)	155	165	200
SqueezeNeRF (512 cache)	39	168	202

Table 3. **Results: cache-size and inference speed.** SqueezeNeRF cache-size and inference speed of the 800x800 images from synthetic 360° scene. The inference speed has been reported on two different GPUs - Nvidia V100 and Nvidia A100.

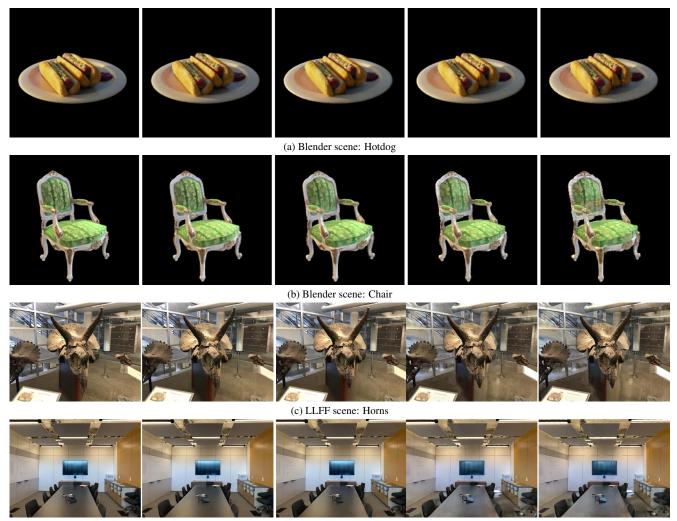| Method	Time [sec] ↓
FastNeRF (1K cache) [6]	420
NeRF-SH (PlenOctree) [18]	1539
SqueezeNeRF (1K cache)	9

Table 4. **Results: Cache generation time on a single Nvidia V100 GPU.** Comparison of time required to cache the trained neural network into a sparse 3D grid (for FastNeRF) or Octree (for PlenOctree) or dense 2D grid (for SqueezeNeRF).

Configuration	PSNR [dB] ↑
NeRF [12]	26.80
SqueezeNeRF (No-cache): 256 hidden units, D=8, weighted combination Eq. (3)	26.92
128 hidden units, $D = 8$, using Eq. (3)	25.61
256 hidden units, $D = 6$, using Eq. (3)	26.31
256 hidden units, $D = 10$, using Eq. (3)	26.67
256 hidden units, $D = 8$, without Eq. (3)	24.11
$n_p = 1024, n_d = 64$ (cache-size=155MB)	26.68
$n_p = 1024, n_d = 32$ (cache-size=155MB)	26.46
$n_p = 512, n_d = 64$ (cache-size=39MB)	24.52
$n_p = 512, n_d = 32$ (cache-size=39MB)	24.42

Table 5. **Results: Other experiments and ablation study.** Comparison of Image quality (in PSNR) of the different SqueezeNeRF configurations for the "Chair" scene in synthetic 360° dataset. In the first row, we report NeRF performance as a reference.

5. Summary and Limitations

We present SqueezeNeRF, a further factorized variation of FastNeRF [6] that allows real-time rendering of NeRF [12] in a memory efficient manner. Similar to the state of the art methods, FastNeRF and NeRF-SH [18], our method also relies on storing a cache of the neural network mapping so that during inference we can replace the millions of neural network computations by simple look-up operations. But while these method can also render at over 150 frames per second, their cache-size, even though they store a sparse version of it, is in the order of few GBs which is a major drawback for any embedded systems application. Our proposed model factorizes the NeRF MLPs into a view conditioned network which takes the camera viewing direction (θ, ϕ) as input and three position conditioned networks, which take $(x, y), (y, z)$ and (z, x) as input respec-

(a) Blender scene: Hotdog

(b) Blender scene: Chair

(c) LLFF scene: Horns

(d) LLFF scene: Room

Figure 3. **Results: Images generated from a novel view in the test set.** From left to right: Ground truth image from the test set, NeRF generation, SqueezeNeRF (no-cache) generation, SqueezeNeRF (1K-cache) generation, SqueezeNeRF (512-cache) generation

tively. This factorization allows us to reduce the memory complexity of our neural network cache from $\mathcal{O}(n^3)$ (for FastNeRF) to $\mathcal{O}(n^2)$. This allows us to store a dense cache which occupies less than 160MB and still enables us to render over 160 frames per second with Nvidia V100 and over 200 frames per second with Nvidia A100.

Despite being competitive with the state of the art models in rendering speed with a considerably less memory overhead, the quality of images generated via cache based inference of our approach is inferior to NeRF and some of the other baselines. This can be attributed to our relatively simple combination scheme of fusing the intermediate outputs as described by Eq. (4). A more sophisticated fusion of these intermediate output or incorporation of training techniques from some other follow-up works on NeRF such as [5, 13, 20] should lead to higher quality of rendered im-

ages. Another point to worth noting is that our factorization scheme, while applied to the position dependent network of FastNeRF in this work, also lends itself for future application to NeRF-SH and SNeRG [7] in a similar manner.

References

[1] Alex Yu and Sara Fridovich-Keil, Matthew Tancik, Qinhong Chen, Benjamin Recht, and Angjoo Kanazawa. Plenoxels: Radiance fields without neural networks, 2021. 1

[2] Yuan Chang and Guo-Ping Wang. A review on image-based rendering. *Virtual Reality & Intelligent Hardware*, pages 39–54, 2019. 1

[3] Shenchang Eric Chen. Quicktime vr: An image-based approach to virtual environment navigation. In *SIGGRAPH*, page 29–38, 1995. 1

[4] Shenchang Eric Chen and Lance Williams. View interpolation for image synthesis. In *SIGGRAPH*, page 279–88, 1993. 1

[5] Kangle Deng, Andrew Liu, Jun-Yan Zhu, and Deva Ramanan. Depth-supervised nerf: Fewer views and faster training for free. *arXiv:2107.02791*, 2021. 1, 8

[6] Stephan J. Garbin, Marek Kowalski, Matthew Johnson, Jamie Shotton, and Julien Valentin. Fastnerf: High-fidelity neural rendering at 200fps. In *ICCV*, 2021. 2, 3, 4, 5, 6, 7

[7] Peter Hedman, Pratul P. Srinivasan, Ben Mildenhall, Jonathan T. Barron, and Paul Debevec. Baking neural radiance fields for real-time view synthesis. *ICCV*, 2021. 2, 3, 5, 6, 7, 8

[8] Ruofan Liang, Hongyi Sun, and Nandita Vijaykumar. Coordx: Accelerating implicit neural representation with a split mlp architecture. In *ICLR*, 2022. 2, 3

[9] David B. Lindell, Julien N. P. Martel, and Gordon Wetzstein. Autoint: Automatic integration for fast neural volume rendering. *CVPR*, pages 14551–60, 2021. 2, 6, 7

[10] Lingjie Liu, Jiatao Gu, Kyaw Zaw Lin, Tat-Seng Chua, and Christian Theobalt. Neural sparse voxel fields. *NeurIPS*, 2020. 2

[11] Ben Mildenhall, Pratul P. Srinivasan, Rodrigo Ortiz-Cayon, Nima Khademi Kalantari, Ravi Ramamoorthi, Ren Ng, and Abhishek Kar. Local light field fusion: Practical view synthesis with prescriptive sampling guidelines. *TOG*, 2019. 5

[12] Ben Mildenhall, Pratul P. Srinivasan, Matthew Tancik, Jonathan T. Barron, Ravi Ramamoorthi, and Ren Ng. Nerf: Representing scenes as neural radiance fields for view synthesis. In *ECCV*, 2020. 1, 2, 3, 5, 6, 7

[13] Thomas Neff, Pascal Stadlbauer, Mathias Parger, Andreas Kurz, Joerg H. Mueller, Chakravarty Reddy Alla Chaitanya, Anton Kaplanyan, and Markus Steinberger. Donerf: Towards real-time rendering of compact neural radiance fields using depth oracle networks. *Computer Graphics Forum*, 40, 2021. 3, 8

[14] Christian Reiser, Songyou Peng, Yiyi Liao, and Andreas Geiger. Kilonerf: Speeding up neural radiance fields with thousands of tiny mlps. In *ICCV*, 2021. 2, 3, 6, 7

[15] Zhou Wang, A.C. Bovik, H.R. Sheikh, and E.P. Simoncelli. Image quality assessment: from error visibility to structural similarity. *TIP*, pages 600–12, 2004. 5

[16] Suttisak Wizadwongsa, Pakkapon Phongthawee, Jiraphon Yenphraphai, and Supasorn Suwajanakorn. Nex: Real-time view synthesis with neural basis expansion. In *CVPR*, 2021. 2, 3, 6

[17] Liwen Wu, Jae Yong Lee, Anand Bhattad, Yuxiong Wang, and David Forsyth. Diver: Real-time and accurate neural radiance fields with deterministic integration for volume rendering. *arXiv:2111.10427*, 2021. 2, 3, 6, 7

[18] Alex Yu, Ruilong Li, Matthew Tancik, Hao Li, Ren Ng, and Angjoo Kanazawa. Plenoctrees for real-time rendering of neural radiance fields. In *ICCV*, 2021. 2, 3, 5, 6, 7

[19] Alex Yu, Vickie Ye, Matthew Tancik, and Angjoo Kanazawa. pixelnerf: Neural radiance fields from one or few images. In *CVPR*, pages 4578–87, 2021. 1

[20] Kai Zhang, Gernot Riegler, Noah Snavely, and Vladlen Koltun. Nerf++: Analyzing and improving neural radiance fields. *arXiv:2010.07492*, 2020. 1, 8

[21] R. Zhang, P. Isola, A. A. Efros, E. Shechtman, and O. Wang. The unreasonable effectiveness of deep features as a perceptual metric. In *CVPR*, pages 586–95, 2018. 5